Coordination Chemistry Reviews 254 (2010) 1628–1636

Contents lists available at ScienceDirect

Coordination Chemistry Reviews

journal homepage: www.elsevier.com/locate/ccr

Review

Template synthesis of azacyclam metal complexes using primary amides as locking fragments

Luigi Fabbrizzi*, Maurizio Licchelli, Lorenzo Mosca, Antonio Poggi

Dipartimento di Chimica Generale, Università di Pavia, via Taramelli 12, 27100 Pavia, PV, Italy

Contents

1. Metal template syntheses 1628
2. Azacyclam complexes 1630
3. Multicentered redox systems 1631
4. Redox switches of fluorescence 1632
5. The interaction with anions: acetate 1633
6. Conclusion 1636
Acknowledgements 1636
References 1636

ARTICLE INFO

Article history:
Received 25 September 2009
Accepted 1 December 2009
Available online 5 December 2009

Keywords:
Template syntheses
Macrocycles
Nickel(III) complexes
Molecular switches
Anion receptors

ABSTRACT

Nickel(II) and copper(II) azacyclam complexes can be obtained through a metal template procedure involving the pertinent open-chain tetramine, formaldehyde and a primary amide (either carboxy- or sulfonamide) as a locking fragment. Azacyclam complexes, which display the same properties and solution behavior of the corresponding cyclam analogues, can be obtained with any desired side-chain appended to the ligand's framework, by choosing the appropriate amide derivative, through a convenient one-pot synthesis. This opens the way to the design of multi centered redox systems, redox switches of fluorescence, and anion receptors of unusually high Brønsted acidity.

© 2009 Elsevier B.V. All rights reserved.

1. Metal template syntheses

Metal ions typically interact with molecules displaying binding tendencies (ligands) and place them in the space around themselves, according to a definite geometrical order. This property lies at the basis of coordination chemistry and, over the last 100 years, gave rise to thousands and thousands of compounds of interest for medical care, diagnostics, industrial catalysis, optics and electronics, solar energy harvesting, hydrometallurgical extraction, *et cetera* [1]. In some particular cases, metal coordinated ligands react with molecules coming from the solution to give a ligand of higher denticity, whose structure still satisfies the geometrical requirements of the metal center and which can reach a high level of sophistication. The metal addresses the synthetic pathway to a chemical object of a predetermined geometry and is said to act as a *template*. The term template was first used in chemistry by Busch and Thompson, to illustrate the role of nickel(II) in the synthesis of macrocyclic complexes like **2** (see Scheme 1) [2].

In fact, the Ni^{II} ion, which has a pronounced preference for square coordination, places and orientates the two thiolate sulphur atoms in positions favorable to the reaction with one molecule of 1,2-bis(bromomethyl)benzene, thus affording the synthesis of the macrocyclic complex **2** with a 60% yield. Notice that the cyclization process – which involves the stepwise nucleophilic attack of a thiolate sulphur atom on a $BrCH_2$– group – is intrinsically irreversible. Things go better, and yields can become higher, when the cyclization process is reversible. One of the first examples in this sense was provided by Karn and Busch with the synthesis of the nickel(II) tetra-aza-macrocyclic complex, shown in Scheme 2 [3].

First, Ni^{II} forms a 1:1 complex with the open-chain triamine **3**, picking up one water molecule from the solution to achieve four-coordination according to a square geometry (**4**). Then, in step (ii), the sp^2 nitrogen atom of a 2,6-diacetylpyridine molecule displaces the labile water molecule and binds the Ni^{II} center, thus bringing the two carbonyl groups within reaction distance of the two primary amine groups of the coordinated triamine. At this stage,

* Corresponding author. Tel.: +39 0382 987328; fax: +39 0382 528544.
E-mail address: luigi.fabbrizzi@unipv.it (L. Fabbrizzi).

0010-8545/$ – see front matter © 2009 Elsevier B.V. All rights reserved.
doi:10.1016/j.ccr.2009.12.002

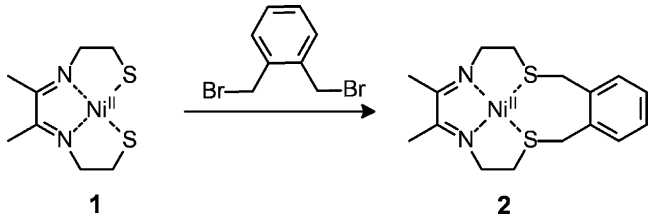

Scheme 1. The first metal template synthesis of a macrocycle. The Ni^{II} ion places the two thiolate sulphur atoms in positions suitable for cyclization, which involves the irreversible nucleophilic attack on the $BrCH_2$– groups of 1,2-bis(bromomethyl)benzene.

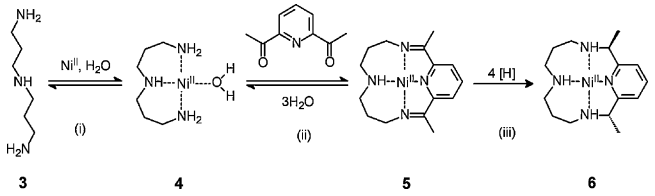

Scheme 2. The nickel(II) template synthesis of CR (**5**) and CRH (**6**) tetra-aza-macrocyclic complexes. The cyclization step (ii) involves the reversible Schiff base condensation of the carbonyl groups of 2,6-diacetylpyridine with the $–NH_2$ groups of the triamine **3**, preoriented through coordination to the metal.

a Schiff base condensation reaction takes place and a tetra-aza macrocycle is formed. The formation of the C=N imine bond is reversible, as it can undergo fast hydrolysis to give back the ketone and the amine. Reversibility guarantees, through a trial and error mechanism, the achievement of the most stable structural arrangement, in the present case the formation of the 14-membered tetra-aza macrocycle. The coordinative situation can be 'frozen' (i.e. the hydrolysis of the imine bond prevented) by hydrogenating the two C=N fragments [4], giving complex **6**. Complexes **5** and **6** are currently indicated as $[Ni^{II}(CR)]^{2+}$ and $[Ni^{II}(CRH)]^{2+}$, respectively [5]. Two diastereoisomers are formed, depending whether the two methyl substituents extend on either the same or opposite sides of the plane of the complex: *meso* (*R*,*S*) or racemic (*R*,*R* + *S*,*S*), respectively. The meso (red) and racemic (yellow) complexes are obtained according to a 10:1 ratio. Both complexes are diamagnetic, a spin state of Ni^{II} that corresponds to the formation of complexes of square coordination geometry. Structural features and configurational details of the two diastereoisomers were later made clear through the determination of crystal and molecular structures [8,9]. In particular, Fig. 1 shows the structures of the nickel(II) complexes with the *R*,*S* form and the *R*,*R* enantiomer of CRH. Both complexes can be demetalated with excess cyanide to give the free ligands.

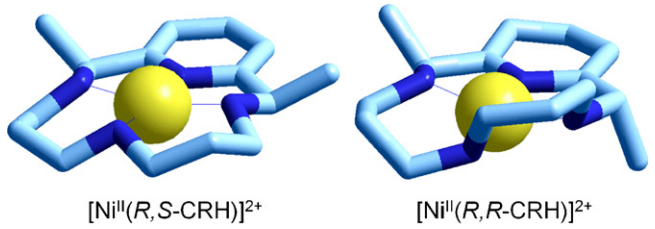

Fig. 1. The molecular structure of the Ni^{II} complexes of CRH (2,12-dimethyl-3,7,11,17-tetra-azabicyclo1[1.3.1]heptadeca-1(17),13,15-triene). Due to the presence of two asymmetric carbon atoms, the tetra-aza ligand gives rise to two diastereoisomers: the (*R*,*S*) meso form, with the two methyl groups on the same side of the plane of the complex and the racemic (*R*,*R* + *S*,*S*) form, with the methyl groups in the opposite sides. The *R*,*S* (meso) configuration allows the establishing of stronger metal–ligand interactions, according to a less distorted square geometry, which accounts for the higher thermodynamic stability. Structures redrawn from data deposited at the Cambridge Crystallographic Data Centre: *R*,*R*, Ref. [8]; *R*,*S* Ref. [9].

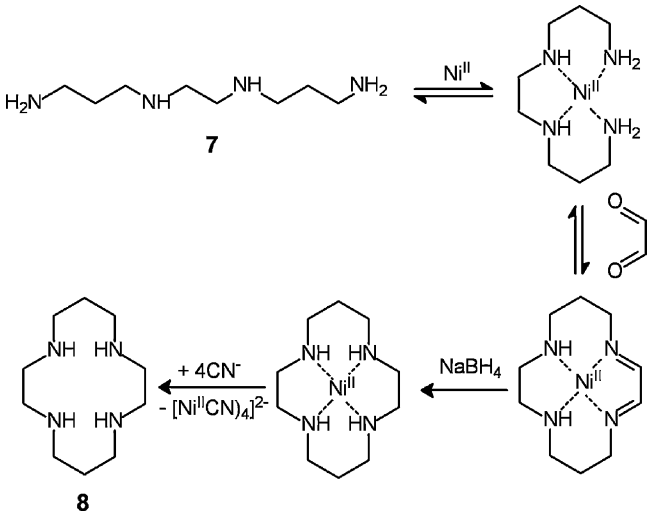

Scheme 3. The nickel(II) template synthesis of cyclam, 1,4,8,11-tetra-aza-cyclotetradecane (**8**) [10]. The cyclization step involves the reversible Schiff base condensation of the carbonyl groups of glyoxal with the $–NH_2$ groups of the linear tetramine **7**, preoriented through coordination to the metal.

CRH transition metal complexes profit from the benefits of the coordination by a 14-membered tetra-aza-macrocycle: high thermodynamic and kinetic stability, which is expressed for instance by a high resistance to the demetalation by strong acids. However, the most pronounced macrocyclic properties are observed with cyclam (**8**), which possesses four secondary amine nitrogen donor atoms and, on complexation, gives an alternating sequence of five- and six-membered chelate rings. Cyclam is obtained through a Ni^{II} template synthesis [10], and, also in this case, the cyclization step involves a Schiff base condensation, as illustrated in Scheme 3.

Cyclam has a pronounced tendency to stabilize unusually high oxidation states of the encircled metal [11]. For instance, the stable yellow $[Cu^{III}(cyclam)]^{3+}$ complex can be obtained through chemical (with $S_2O_8^{2-}$) or electrochemical oxidation of the corresponding Cu^{II} complex in a strongly acidic solution [12]. The $[Ag^{II}(cyclam)]^{2+}$ complex has been isolated in a crystalline form and its structure has been elucidated through X-ray diffraction experiments [13]. Moreover, $[Ag^{II}(cyclam)]^{2+}$ undergoes reversible oxidation in water to give the stable $[Ag^{III}(cyclam)]^{3+}$ species [14]. $[Hg^{III}(cyclam)]^{3+}$ has been electrochemically generated as a red transient and characterized in the cavity of an ESR spectrometer [15]. However, the most investigated uncommon oxidation state among transition metal cyclam complexes is Ni^{III}, d^7 low-spin, showing a preference towards axially elongated octahedral geometry [16]. Indeed, Ni^{III} cannot be any longer regarded as a rather uncommon oxidation state, if one considers that the $Ni^{III}(cyclam)]^{3+}/Ni^{II}(cyclam)]^{2+}$ couple in 1 M HCl has an electrode potential of 0.71 V vs. NHE, i.e. less positive than that corresponding to the Fe^{3+}/Fe^{2+} couple under the same conditions (0.77 V vs NHE) [17]. For this reason, the $Ni^{II}(cyclam)^{2+}$ moiety has been used as a redox active unit in the design of multicomponent systems, as a sort of inorganic analogue of ferrocene (Fc, easily oxidizable to Fc^+), and it has been appended to a variety of organic substrates in order to generate functional systems (simple molecular devices [18], electrochemical sensors [19], and anion carriers through liquid membranes [20]). The design of the pertinent multicomponent systems requires the derivatization of the redox subunit, a task easily performed in the case of ferrocene, prone to substitution reactions at the aromatic ring. On the contrary, in the case of cyclam, derivatization has to be carried out at one of the amine nitrogen atoms of the demetalated ligand and requires selective protection, functionalization, deprotection, then complex formation. Moreover, the obtained Ni^{II}

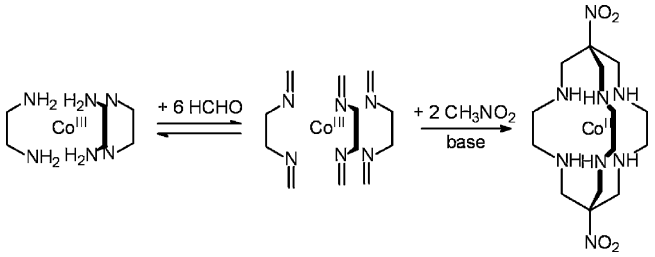

Scheme 4. The synthesis of the $[Co^{III}(diNOsar)]^{3+}$ complex (diNOsar = dinitrosarcophagine) [23]. CH_3NO_2 can be replaced by the other triprotic acid NH_3 to give the $[Co^{III}(sepulchrate)]^{3+}$ complex [22].

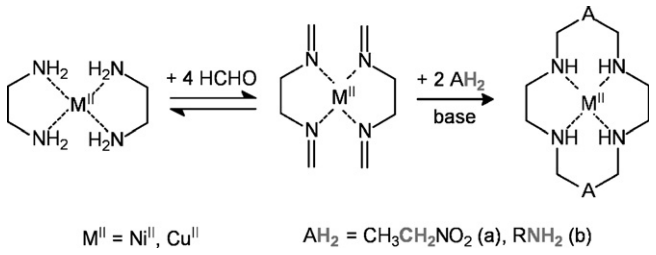

Scheme 5. The synthesis of cyclam-like macrocyclic complexes, from bis-ethylenediamine complexes of Cu^{II} and Ni^{II}, in the presence of formaldehyde and base, using a diprotic acid AH_2 as a locking fragment.

complex contains a tertiary amine group, a circumstance which alters the redox properties, in particular making more difficult the attainment of the Ni^{III} state [21]. Fortunately, there exists a template procedure that allows the one-pot synthesis of cyclam-like Ni^{II} (and Cu^{II}) complexes, bearing on their organic backbone any desired functionalization. Such a template synthesis refers to the so-called azacyclam complexes, whose distinctive properties will be discussed in the next Sections.

2. Azacyclam complexes

A further convenient route to cyclam-like macrocyclic complexes was inspired by Sargeson's classical template syntheses of Co^{III} sepulchrate and sarcophagine (sar) complexes, illustrated in Scheme 4 [22,23]. In the one-pot syntheses of these cage complexes, first six molecules of formaldehyde undergo Schiff base condensation with the primary amine groups of a $[Co^{III}(en)_3]^{3+}$ complex (en: 1,2-diaminoethane), then two molecules of a triprotic acid (NH_3 [22] and CH_3NO_2 [23], respectively), in the presence of base, deprotonate stepwise. Then, the corresponding anions consecutively attack the imine bonds, to give macropolycyclization (see Scheme 4).

If a *triprotic* acid, e.g. nitromethane, $\mathbf{CH_3}NO_2$, is required to accomplish tridimensional polycyclization, a *diprotic* acid, e.g. nitroethane, $CH_3\mathbf{CH_2}NO_2$, should afford cyclization in the two dimensions, to give a macrocylic complex. Following this approach, Sargeson et al. reported the reaction of two molecules of nitroethane ($CH_3\mathbf{CH_2}NO_2$) with $[Cu^{II}(ethylenediamine)_2]^{2+}$, in the presence of formaldehyde and base, to give a dinitrocyclam complex (see Scheme 5, route a) [24].

Then, Suh used a primary amine as a diprotic acid ($CH_3\mathbf{NH_2}$, $C_2H_5\mathbf{NH_2}$), whose reaction with either $[Ni^{II}(en)_2]^{2+}$ or $[Cu^{II}(en)_2]^{2+}$ (en = ethylenediamine) gave diazacyclam complexes (see Scheme 5, route b) [25]. Both Cu^{II} and Ni^{II} ions could be used as a template in view of their tendency to form stable square complexes with two en molecules. Similarly, we observed that another diprotic acid, the $-NH_2$ group of amides, both carboxyamides, $RC(O)NH_2$, and sulfonamides, $RS(O_2)NH_2$, can work as a locking fragment in the synthesis of Cu^{II} [26], and Ni^{II} azacyclam complexes [27], as illustrated in Scheme 6.

As an example, Fig. 2a shows the structure of the Cu^{II} sulfonazacyclam complex, obtained through a template reaction involving methylsulfonamide as a locking fragment [26].

Fig. 2b displays, for comparative purposes, the molecular structure of the $[Cu^{II}(cyclam)]^{2+}$ analogue [28]. In both complexes, the 14-membered tetramine ring is present as the *R,S,S,R* diastereoisomer (also indicated as *trans-III* form) [29], the most stable and most frequently observed configurational isomer of metal complexes of the cyclam ligand [30]. However, the two complexes show subtle, still significant, geometrical differences: for instance, Cu–N

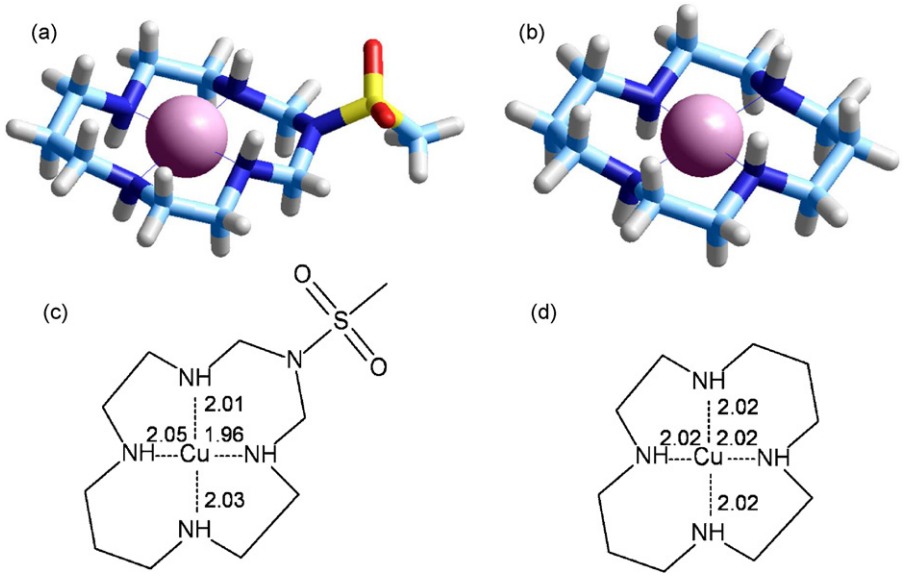

Fig. 2. (a) The molecular structure of the Cu^{II} complex Mesulfonazacyclam [25]; the two NO_3^- counter-ions have been omitted for clarity: they lie in the axial positions of a highly elongated octahedron, with Cu–O distances of 2.53 Å and 2.56 Å; (b) the molecular structure of the Cu^{II} complex of cyclam [28]; the two ClO_4^- counter-ions have been omitted for clarity: they lie in the axial positions of a highly elongated octahedron, with a Cu–O distances of 2.57 Å; (c) Cu-N distances (Å) in the Cu^{II} complex Mesulfonazacyclam; (d) Cu-N distances (Å) in the Cu^{II} complex of cyclam. Structures (a) and (b) redrawn from data deposited at the Cambridge Crystallographic Data Centre: (a) Ref. [26] and (b) Ref. [28].

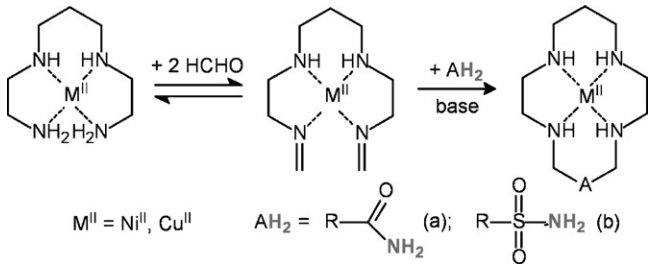

Scheme 6. The metal template synthesis of azacyclam complexes, from complexes of Cu^{II} and Ni^{II} with a linear tetramine, in the presence of formaldehyde and base, using either a carboxyamide or a sulphonamide as a locking fragment.

distances are the same in the cyclam complex (see Fig. 2d), but vary over the 1.96–2.05 Å range in the sulfonazacyclam counterpart. Moreover, in the cyclam complex, the Cu^{II} ion is perfectly coplanar with the four coordinated nitrogen atoms, whereas in the sulfonazacyclam analogue the metal center is displaced by 0.014 Å from the plane of the four amine nitrogen atoms. The deviations from the preferred square coordination geometry in the $[Cu^{II}(Mesulfonazacyclam)]^{2+}$ complex may originate from the presence in the ligand's backbone of a sulfonamide nitrogen atom. The distance of such an atom from the plane described by the two adjacent carbon atoms and by the sulfur atom is 0.156 Å, while for a perfectly tetrahedral atom the distance from the triangle described by three atoms at a bond distance of 1.45 Å should be 0.483 Å. This indicates a definite planarization of the sulfonamide nitrogen atom, to be ascribed to a pronounced π delocalization of the lone pair over the sulfonamide group. It is probably such a distortion that induces subtle deviations of the bonding parameters from those observed in the cyclam complexes. In any case, azacyclam complexes exhibit typical macrocyclic properties, including the extreme resistance to demetalation in strongly acidic solutions. As an example, the $[Cu^{II}(Mesulfonazacyclam)]^{2+}$ complex persists indefinitely in a 1 M $HClO_4$ solution. A striking difference between cyclam and azacyclam complexes refers to the stability of the metal-free macrocycle: the $[Ni^{II}(cyclam)]^{2+}$ complex can be demetalated in a boiling solution of CN^- and separated through liquid–liquid extraction, to eventually give a white crystalline product [10b]. On the other hand, cyanide demetalation of any kind of Ni^{II} azacyclam complexes gave decomposition products, due to the intrinsic instability of the –NH–CH_2–N< system within the azacyclam framework.

3. Multicentered redox systems

The template synthesis of azacyclam provides the unique opportunity to synthesize in one-pot Cu^{II} and Ni^{II} cyclam-like metal complexes bearing as a side-chain any desired functionalization. In fact, given a desired fragment R, it is always possible to obtain its amide derivative, in particular sulfonamide, $RS(O_2)NH_2$, which can be used as a locking fragment in the preparation of the corresponding Ni^{II} or Cu^{II} azacyclam complex. For instance, on reaction of $[Ni^{II}(2,3,2\text{-tet})]^{2+}$ with 1-ferrocenesulfonamide, the conjugate system $[\mathbf{9}]^{2+}$ was obtained [31], which contains two distinct and non-equivalent redox active subunits: $Ni^{II}(cyclam)^{2+}$ (prone to the Ni^{II}/Ni^{III} oxidation process) and ferrocene, Fc (active through the Fc/Fc^+ couple).

Cyclic voltammetry (CV) studies on an MeCN solution of the Ni^{II}(sulfonazacyclam)-ferrocene conjugate $[\mathbf{9}]^{2+}$ disclosed two fully reversible waves: the less anodic peak corresponded to the one-electron oxidation of the ferrocene moiety (Fc/Fc^+), while the more anodic one was ascribed to the one-electron oxidation of the $Ni^{II}(sulfonazacyclam)^{2+}$ subunit (Ni^{II}/Ni^{III} change).

In the diagram in Fig. 3 the $E_{1/2}$ values obtained are compared to the $E_{1/2}$ values pertinent to the 'separate components': 1-ferrocenesulfonamide (**11**) and the Ni^{II} complex of 4-toluenesulfonazacyclam ($[\mathbf{12}]^{2+}$).

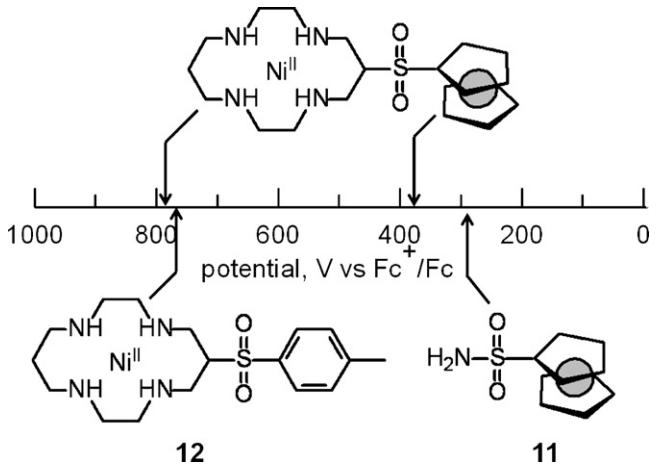

Fig. 3. Half-wave potentials ($E_{1/2}$ vs. Fc^+/Fc in an MeCN 0.1 M in $[Bu_4N]ClO_4$, at 25 °C) associated to the reversible oxidation of the conjugate system $[\mathbf{9}]^{2+}$ and of its 'separate components' **11** and $[\mathbf{12}]^{2+}$. Data from Ref. [31].

It is observed that the oxidation of the ferrocene moiety within the heterodimetallic complex $[\mathbf{9}]^{2+}$ takes place at a potential ca. 80 mV more positive than for the reference system 1-ferrocenesulfonamide (**11**). This may be due to the electrostatic repulsive effect exerted by the proximate dipositive cation (Ni^{II}). On the other hand, the oxidation of the $Ni^{II}(sulfonazacyclam)^{2+}$ fragment of $[\mathbf{9}]^{2+}$ takes place at a potential only slightly more positive than observed for the model system $Ni^{II}(4\text{-toluenesulfonazacyclam})^{2+}$ ($[\mathbf{12}]^{2+}$) This may be ascribed to the fact that the charge increase of the metal centre occurs under the electrostatic repulsion exerted by a monopositive charge, that of the ferrocenium moiety. It should be noticed that the ferrocenesulfonaza subunit, both in the heterodimetallic system $[\mathbf{9}]^{2+}$ and in the model compound **11** undergoes one-electron oxidation at a potential distinctly more positive than plain ferrocene (which, in fact, has been used as an internal reference). This reflects the electron-withdrawing effect exerted by the sulfonamide substituent. In any case, system $[\mathbf{9}]^{2+}$ represents a two-electron redox agent which is active through two unequivalent centers.

The three-component redox active system $[\mathbf{10}]^{2+}$, containing two unequivalent ferrocene subunits and $Ni^{II}(sulfonazacyclam)^{2+}$ moiety, was obtained through the synthetic route illustrated in Scheme 7, which still involves a template process [32].

The redox behavior of $[\mathbf{10}]^{2+}$ was investigated by cyclic voltammetry studies in MeCN solution, made 0.1 M in $[Bu_4N]ClO_4$, at a platinum working electrode. The solid line in Fig. 4 illustrates the CV profile taken for a 10^{-3} M solution of $[\mathbf{10}]^{2+}$ (perchlorate salt), at a potential scan rate of 200 mV s^{-1}.

The profile displays two quasi-reversible oxidation waves, at 0.0 V and 0.31 V, followed by an irreversible and ill-defined peak at ca. 0.8 V. In order to assign unambiguously the observed peaks to the actual redox events, a CV experiment was carried out on a solution 10^{-3} M in (i) plain ferrocene, (ii) 1-ferrocenesulfonamide (**11**) and (iii) $[Ni^{II}(4\text{-toluenesulfonazacyclam})]^{2+}$ ($[\mathbf{12}]^{2+}$). The CV profile (dashed line in Fig. 4) showed three fully reversible waves ($E_{1/2}$ values at: 0.00 V, 0.28 V and 0.79 V vs. Fc^+/Fc, respectively), which are ascribed, in sequence, to the oxidation of plain ferrocene, of 1-ferrocenesulfonamide (**11**) and of $[Ni^{II}(4\text{-toluenesulfonazacyclam})]^{2+}$ ($[\mathbf{12}]^{2+}$). Noticeably, the two less anodic waves of the dashed-line profile coincide with those appearing in the solid line profile, thus indicating that, in the three-component system $[\mathbf{10}]^{2+}$, the first two oxidation steps involve

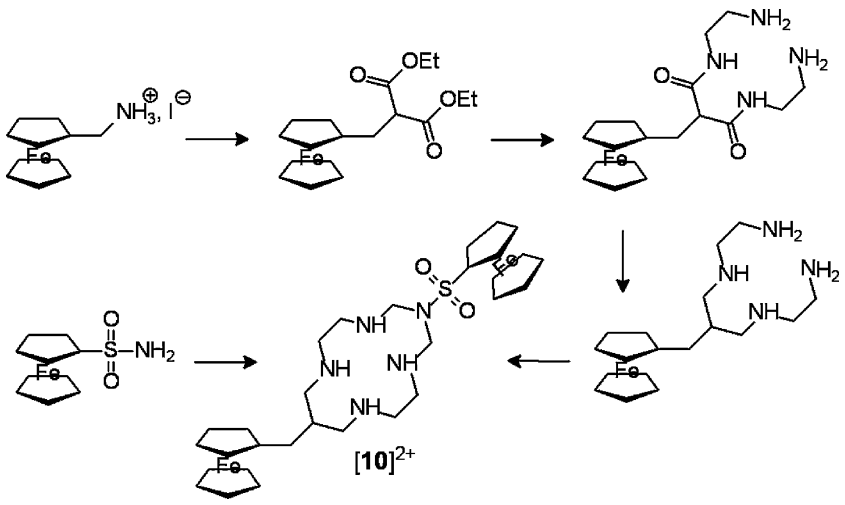

Scheme 7. Synthetic route to the three-component system $[\mathbf{10}]^{2+}$, which contains three unequivalent redox centers [32].

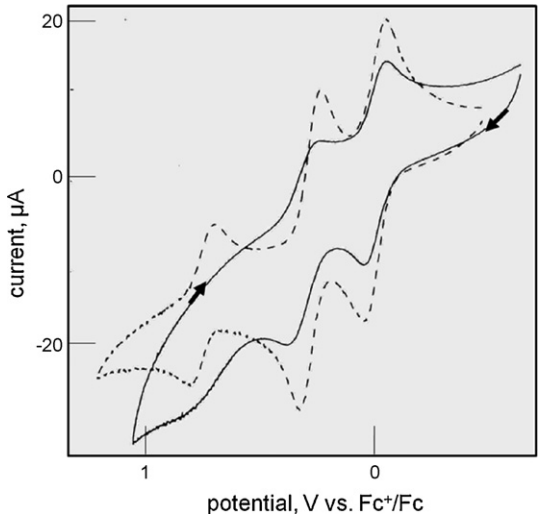

Fig. 4. Cyclic voltammetry profiles obtained at a platinum microsphere for an MeCN solution 0.1 M in $[Bu_4N]ClO_4$. Potential scan rate 200 mV s^{-1}. Solid line: solution 10^{-3} M in $[\mathbf{10}]^{2+}$ (as a perchlorate salt); dashed line: solution 10^{-3} M in plain ferrocene, 1-ferrocenesulfonamide (**11**) and $[Ni^{II}(4\text{-toluenesulfonazacyclam})]^{2+}$ ($[\mathbf{12}]^{2+}$). Figure adapted from Ref. [32].

the two ferrocene subunits. Repulsive electrostatic effects are minimized due to the large distance between the two ferrocene subunits, so that $E_{1/2}$ values coincide with those of the 'separate components'. On the other hand, oxidation of the Ni^{II} center seems to generate a very unstable system, due to the occurrence of intense mutual repulsions between the Ni^{III} cation and the proximate ferrocenium subunits, which leads to decomposition and fragmentation.

4. Redox switches of fluorescence

Luminescent fragments can also be appended to a Ni^{II} azacyclam system. For instance, reaction of $[Ni^{II}(2.3.2\text{-tet})]^{2+}$ with dansylamide, gives complex $[\mathbf{13}]^{2+}$, as a crystalline perchlorate salt [33]. Fig. 5 shows the crystal structure of the complex, which has been recrystallized from an acidic solution, in which the aniline nitrogen atom is protonated.

The dansyl fragment, in the conjugate system $[\mathbf{13}]^{2+}$, displays the typical fluorescent behavior of the isolated component dansylamide (Dns). In particular, when excited at 336 nm (the wavelength of the most intense absorption band of the naphthalene fragment), an MeCN solution of $[\mathbf{13}]^{2+}$ shows a non-structured emission band centred at 510 nm, which results from a charge transfer excited state (solid line in Fig. 6).

Cyclic voltammetry studies showed that the Ni^{II} center in the two-component system $[\mathbf{13}]^{2+}$, in an MeCN solution made 0.1 M in Bu_3BzNCl, undergoes one-electron oxidation to the Ni^{III} species, with $E_{1/2}$ = 0.08 V vs. Fc^+/Fc. A green solution of the Ni^{III} derivative can be obtained through a bulk electrolysis experiment, by setting the potential of the working electrode (a platinum gauze) at 0.23 V vs. Fc^+/Fc. Noticeably, the electrolyzed solution is no longer fluorescent, as the dansyl emission band has been almost completely quenched (short-dash line in Fig. 6). However, if the potential of the working electrode is set at −0.07 V, the yellow solution of the Ni^{II} derivative forms again and fluorescence is fully restored (see spectrum in Fig. 6, long-dash line). Thus, the light emission of the dansylamide subunit in the conjugate system $[\mathbf{13}]^{2+}$ can be switched on/off at will, through the Ni^{II}/Ni^{III} couple, by a variation of the electrode potential as an input.

The occurrence of the Dns*-to-Ni^{III} eT process can be accounted for on a thermodynamic basis. In particular, the free energy change associated to the eT process, ΔG°_{eT}, can be calculated through

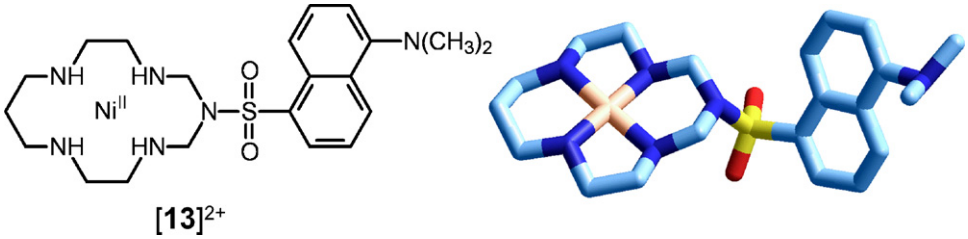

Fig. 5. A Ni^{II} azacyclam complex with an appended fluorophore (dansylamide). The molecular structure refers to the complex in which the aniline nitrogen atom of the dansylamide moiety is protonated. Structure redrawn from data deposited at the Cambridge Crystallographic Data Centre: ref. [33].

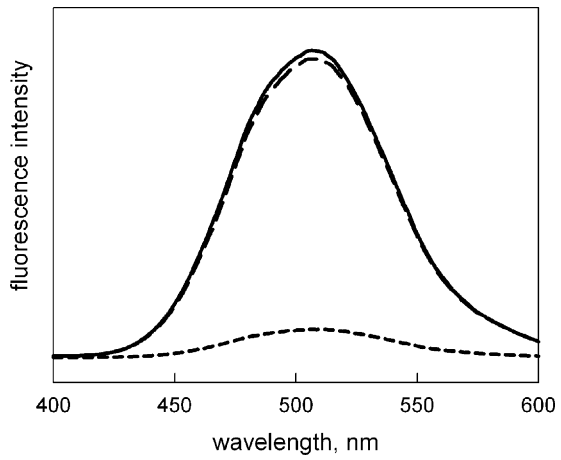

Fig. 6. Redox switching of the fluorescent emission of the dansyl subunit in the two-component system $[\mathbf{13}]^{2+}$. Solid line: emission spectrum of an MeCN solution of the Ni^{II} derivative; short-dash line: emission spectrum of the same solution after exhaustive electrolysis (working electrode potential set at 0.23 V vs. Fc^{+}/Fc): the Ni^{III} derivative is present in solution; long-dash line: emission spectrum of the same solution, which has been electrolysed again at a potential $E = -0.07$ V: the Ni^{II} complex is formed on reduction, and fluorescent emission is fully restored. Figure adapted from Ref. [33].

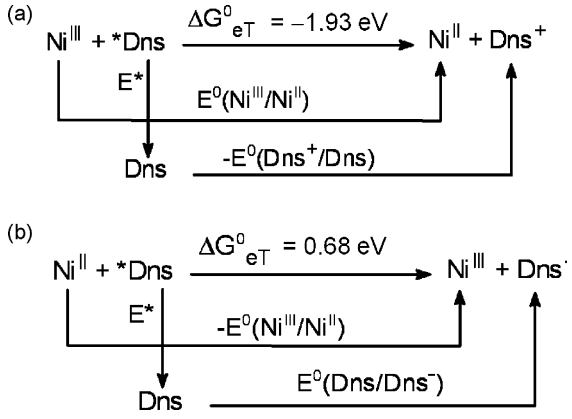

Fig. 7. Thermodynamic cycles for the calculation of the ΔG°_{eT} values associated to: (a) the eT process involving the oxidized form $[\mathbf{13}]^{3+}$ (which takes place, quenching Dns fluorescence) and to (b) the eT process involving the reduced form $[\mathbf{13}]^{2+}$ (which does not take place, so that fluorescence emission is not quenched).

the thermodynamic cycle reported in Fig. 7a, by combining the pertinent photophysical and electrochemical quantities: E^{*}(Dns*), given by the energy of the emission band, $E_{1/2}(Ni^{III}/Ni^{II})$ and $E_{1/2}(Dns^{+}/Dns)$, obtained from the cyclic voltammetry profiles. In the present case, ΔG°_{eT} is distinctly negative, −1.93 eV, thus making the eT process responsible for fluorescence quenching strongly favored (state: off). On the contrary, the occurrence of a Ni^{II}-to-Dns* eT process is thermodynamically prevented ($\Delta G^{\circ}_{eT} = 0.68$ eV), thus accounting for the unperturbed light emission of the reduced form of $[\mathbf{13}]^{2+}$ (state: on; see Fig. 7b).

According to the language of supramolecular chemistry, which often relies on metaphors referring to everyday's life, we are in the presence of a molecular light switch. In fact, in system $[\mathbf{13}]^{2+}$, we can identify the light bulb (the dansylamide fragment), the electrical wire (the N-SO_2 spacer), and the real switch (the nickel-azacyclam subunit). The switch can be operated through an external input (the variation of the electrode potential) and this results in either light emission (switch on) or quenching (switch off). In everyday's life, one wishing to change the type of light simply unscrews the bulb and replaces it with a different one. In the molecular world, the dansyl fragment, emitting in the visible, can be replaced by a plain naphthalene fragment ($[\mathbf{14}]^{2+}$), which gives a genuine π–π^{*} excited state and emits in the UV region ($\lambda_{max} = 360$ nm), by

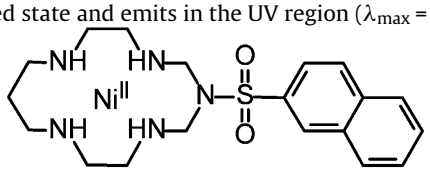

14

using 2-naphthalenesulphonamide as a locking fragment in the Ni^{II} template reaction [33]. Also in the present case, fluorescence can be switched on (Ni^{II})/off (Ni^{III}) through the metal-centered redox couple (the real switch) in a controlled potential electrolysis experiment in a MeCN solution, by varying in a proper way the potential of the platinum gauze, acting as a working electrode.

5. The interaction with anions: acetate

On reaction of $[Cu^{II}(2.3.2\text{-tet})]^{2+}$ with a phenylurea (see Scheme 8), an azacyclam complex bearing a pendant secondary amide group is obtained [34].

Fig. 8 shows the molecular structures of the complexes $[\mathbf{15}]^{2+}$ (a) and $[\mathbf{16}]^{2+}$ (b), which have a nitro- and a cyano-substituent on the phenyl ring, respectively.

Secondary amide groups, activated by electron-withdrawing substituents (e.g. 4-nitrophenyl, 4-cyanophenyl) have been extensively used as hydrogen bonding donors in the design of a variety of neutral anion receptors [35]. On the other hand, the Cu^{II} center, encircled by a tetramine macrocycle, is prone to the interaction with an anion, to give a five-coordinate species. Thus, complexes $[\mathbf{15}]^{2+}$ and $[\mathbf{16}]^{2+}$ can potentially behave as ditopic receptors for anions, providing (i) H-bond interaction at the carboxamide N–H fragment and (ii) metal–ligand interaction at the coordinatively unsaturated Cu^{II} center. In particular, there was a specific interest to assess the existence of any cooperative effect in the interaction of the $[\mathbf{15}]^{2+}$ and $[\mathbf{16}]^{2+}$ complexes with anions. However, in order to establish the individual binding tendencies of each subunit, preliminary studies were carried out on the model systems **17**, **18** and $[\mathbf{19}]^{2+}$.

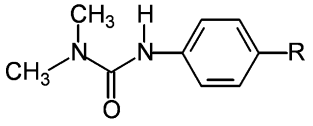

R = NO_2 **17**; R = CN **18**

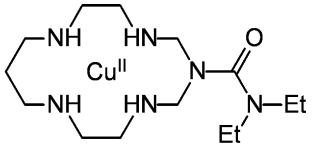

$[\mathbf{19}]^{2+}$

Studies on the hydrogen bonding donating tendencies of neutral receptors (amides, ureas, pyrroles *et cetera*) have to be carried out in

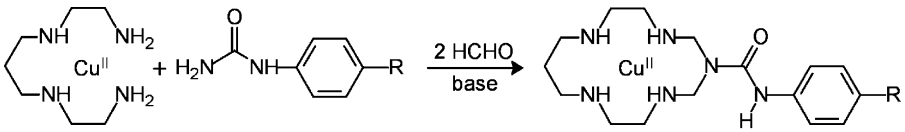

R = NO_2, $[\mathbf{15}]^{2+}$; R = CN, $[\mathbf{16}]^{2+}$

Scheme 8. Template synthesis of Cu^{II} azacyclam complexes bearing a pendant amide group.

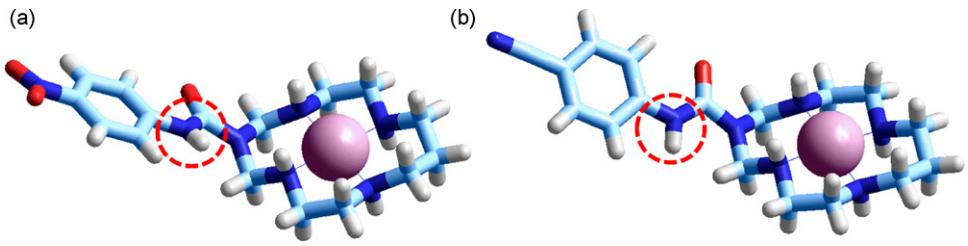

Fig. 8. The molecular structure of $[\mathbf{15}]^{2+}$ and $[\mathbf{16}]^{2+}$ copper(II) complexes bearing a pendant secondary amide group, suitable for the interaction with anions. Structures (a) and (b) redrawn from data deposited at the Cambridge Crystallographic Data Centre: Ref. [34].

aprotic media (typically $CHCl_3$, MeCN, or DMSO), in order to avoid the successful competition by the solvent [36]. In this case, DMSO was chosen as a solvent, as it guaranteed adequate solubility of $[\mathbf{15}](ClO_4)_2$ and $[\mathbf{16}](ClO_4)_2$. Anion binding studies were performed by titrating a solution of the receptor with a standard solution of the anion, in the form of its tetrabutylammonium salt. Amides **17** and **18** show rather intense bands centered at 350 nm (**17**, $\varepsilon = 13400\ cm^{-1}\ M^{-1}$) and at 280 nm (**18**, $\varepsilon = 24400\ cm^{-1}\ M^{-1}$). Each band originates from a charge transfer transition from the nitrogen atom of the amide N–H fragment to the electron-withdrawing substituent (–NO_2 or –CN), along the phenyl ring. It should be noted that the occurrence of the optical transition generates a partial negative charge on the substituent and a partial positive charge on the amide nitrogen atom. Thus, interaction of a negatively charged ion at the N–H fragment is expected to stabilize the excited state, thus reducing the energy of the transition. As a consequence, on interaction with the anion, a red-shift of the absorption band should be observed [37]. The stronger the anion receptor interaction, the more pronounced the red-shift. However, on addition of any anion (acetate, halides), even in a large excess, to a 5×10^{-5} M solution of **17** or **18**, no spectral modifications were observed, which indicated that receptor-anion association constants are lower than 10^2 and demonstrated the poor donating tendencies of a single N–H fragment towards anions. Indeed, the many investigated amide based anion receptors contain several N–H fragments, which have been strategically placed inside a cavity [38]. On the other hand, a DMSO solution of the Cu^{II} complex $[\mathbf{19}]^{2+}$, which does not contain the N–H fragment, shows a d–d band centered at 525 nm, with a molar extinction coefficient $\varepsilon = 85\ M^{-1}\ cm^{-1}$. Likewise, on addition of excess anion to a 5×10^{-3} M DMSO solution of $[\mathbf{19}]^{2+}$, no spectral modifications were observed. This indicates that no anion is able to displace DMSO molecules from the apical positions of the elongated octahedron. On these premises, a DMSO solution of $[\mathbf{16}]^{2+}$ was titrated with a DMSO standard solution of $[Bu_4N]CH_3COO$. Fig. 10 shows the family of spectra recorded over the course of the titration.

Indeed, acetate addition induced drastic spectral changes: in particular, the receptor's band, centered at 270 nm, disappeared, while a new less intense band, centered at 330 nm, formed and developed.

H-bond interactions between anions and the amide N–H fragments red-shift the absorbance by at most 15 nm. In the present case, we observed a red-shift of 60 nm, indicating N–H deprotonation [39,40]. Thus, the occurrence of the following acid–base neutralization equilibrium is suggested:

$$[Cu^{II}(LH)]^{2+} + CH_3COO^- \leftrightarrows [Cu^{II}(L)]^{+} + CH_3COOH \quad (1)$$

Best fitting of spectrophotometric titration data, using a non-linear least-squares procedure and extended over the 250 – 370 nm interval, was obtained on assuming the occurrence of a 1:1 equilibrium, to which a value of $\log K = 4.35 \pm 0.03$ corresponded. Fig. 9b shows the percent concentration of the undeprotonated $[Cu^{II}(LH)]^{2+}$ and deprotonated $[Cu^{II}(L)]^{+}$ systems, calculated on the basis of the $\log K$ value. Occurrence of equilibrium (1) is confirmed by the fact that (i) the absorbance of receptor $[\mathbf{16}]^{2+}$ (e.g. taken at 280 nm) superimposes well on the concentration profile of $[Cu^{II}(LH)]^{2+}$ and (ii) the absorbance of the band at 330 nm superimposes well on the concentration profile of the deprotonated receptor $[Cu^{II}(L)]^{+}$. At this stage, it must be considered that acetate induced deprotonation of an N–H fragment in DMSO had been previously observed in the case of a thiourea derivative, equipped with powerful electron-withdrawing substituents [41]. Thiourea is a distinctly stronger acid than urea, in DMSO (pK_a values: 21.1 and 26.95, respectively [42]). Moreover, in the mentioned case [41], two stepwise equilibria occurred: (i) the formation of a thiourea-acetate H-bond complex, (ii) deprotonation of the N–H fragment, with simultaneous formation of the $[CH_3COOH\cdots CH_3COO]^-$ H-bond self-complex. Quite surprisingly, in the present case, (i) acetate induced deprotonation of the N–H fragment takes place with the less acidic urea subunit, and (ii) it did not involve the formation of the $[CH_3COOH\cdots CH_3COO]^-$ complex, but occurs directly on addition of only 1 equiv. of acetate. This evidence suggested

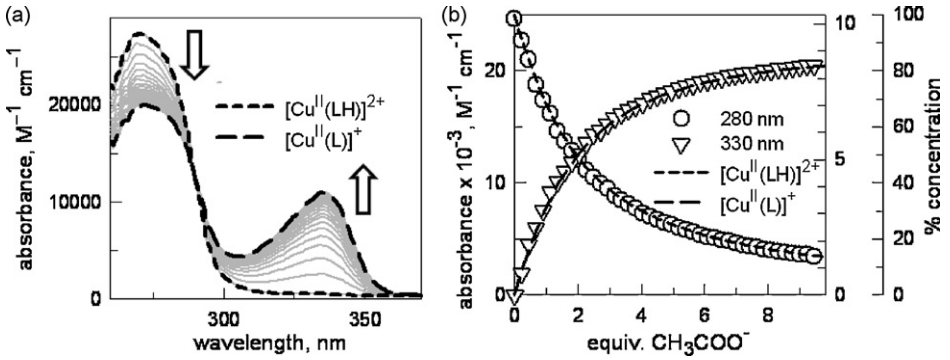

Fig. 9. (a) spectra recorded over the course of the titration of a 5×10^{-5} M solution of the Cu^{II} azacyclam complex $[\mathbf{16}]^{2+}$, indicated in the Figure as $[Cu^{II}(LH)]^{2+}$, in DMSO with a 4.5×10^{-3} M DMSO solution of $[Bu_4N]CH_3COO$; (b) dashed lines: % concentration of the undeprotonated $[Cu^{II}(LH)]^{2+}$ and deprotonated $[Cu^{II}(L)]^{+}$ species (off right vertical axis), (b) symbols: absorbance of the bands centred at 280 nm, $[Cu^{II}(LH)]^{2+}$ (right vertical axis) and at 330 nm, $[Cu^{II}(L)]^{+}$ (left vertical axis). Figure adapted from Ref. [33].

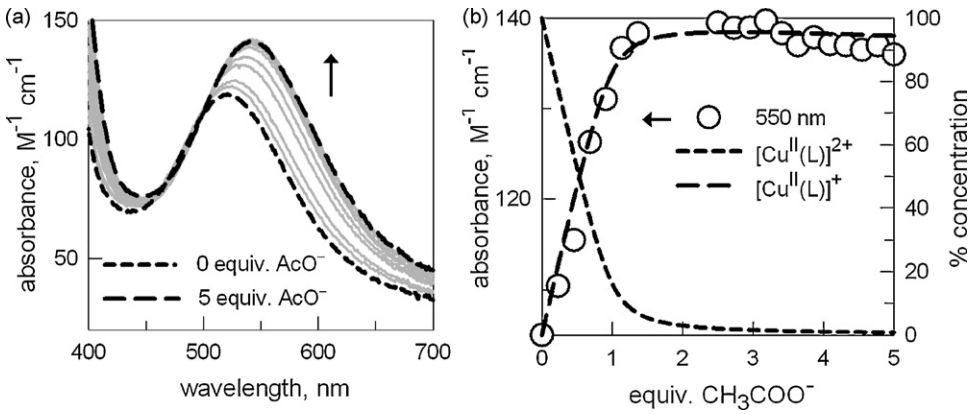

Fig. 10. (a) spectra taken over the course of the titration of a 1.02×10^{-3} M solution of the Cu^{II} azacyclam complex [**16**]$^{2+}$, in DMSO with a 0.102 M DMSO solution of [Bu$_4$N]CH$_3$COO; (b) dashed lines, % concentration of the undeprotonated [Cu^{II}(LH)]$^{2+}$ (short dash) and deprotonated [Cu^{II}(L)]$^{+}$ species (long dash, off right vertical axis), (b) symbols: absorbance of the band centered at 550 nm, pertinent to the [Cu^{II}(L)]$^{+}$ complex (left vertical axis). Figure adapted from Ref. [34].

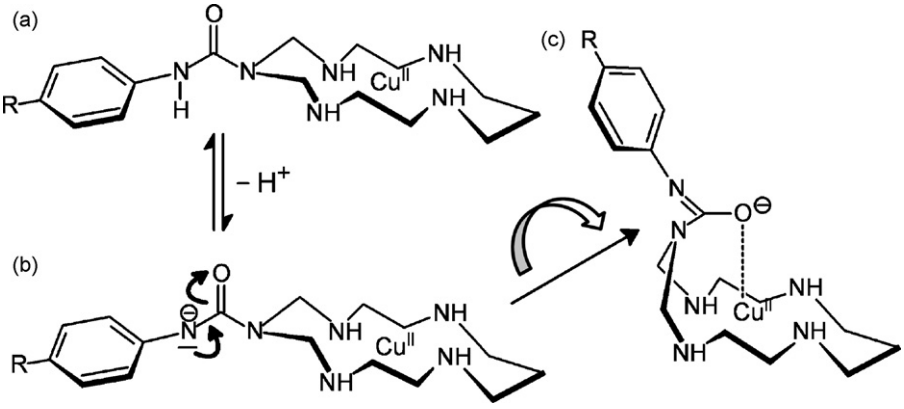

Scheme 9. Metal induced deprotonation of the secondary amide group. The deprotonation process is favored by the coordination to the Cu^{II} centre of the carbonyl oxygen atom, which exhibits a partial negative charge (R = CN, NO$_2$).

the occurrence of a major cooperative effect exerted by the proximate Cu^{II} center. The role of the metal ion was revealed by carrying out a titration experiment on a 20-fold more concentrated solution of [**16**]$^{2+}$, which allowed examination of the d–d band, centered at 550 nm ($\varepsilon = 120\ M^{-1}\ cm^{-1}$). Details of the spectrophotometric titration experiment are illustrated in Fig. 10.

In particular, Fig. 10a shows the d–d spectra taken during the titration of a 1.02×10^{-3} M solution of [**16**]$^{2+}$ in DMSO with [Bu$_4$N]CH$_3$COO. The band centred at 510 nm (short dash in Fig. 10a) is that typically observed for the Cu^{II}(azacyclam)^2 square planar complex (whose coordination geometry is shown in Fig. 8). On acetate addition, (i) the band is shifted to higher wavelength and (ii) it increases in intensity. Such a behaviour is typically observed for copper(II) complexes moving from a square planar geometry to a five-coordination, according to a square pyramidal geometry. Five-coordination cannot be ascribed to an oxygen atom of the CH$_3$COO$^-$, as titration experiments on the model system [**19**]$^{2+}$ have demonstrated that the Cu^{II} center does not display any affinity towards anions in a DMSO solution. Therefore, it is suggested that the fifth donor atom is the carbonyl oxygen atom of the urea sub-

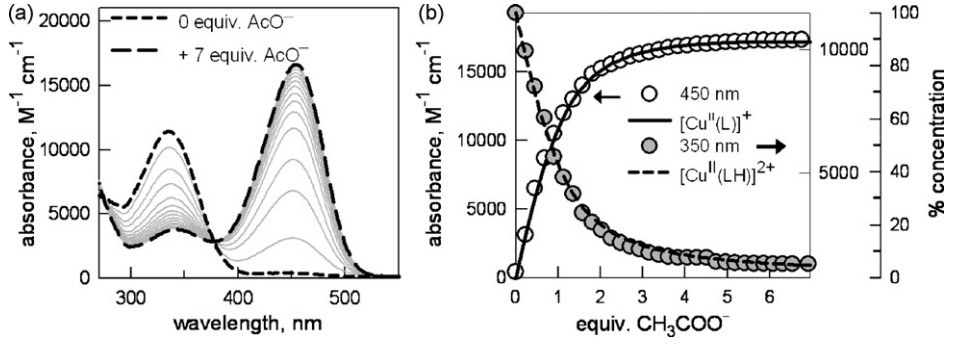

Fig. 11. (a) spectra taken over the course of the titration of a 5×10^{-5} M solution of the Cu^{II} azacyclam complex [**15**]$^{2+}$, in DMSO with a 4.5×10^{-3} M DMSO solution of [Bu$_4$N]CH$_3$COO; (b) dashed line, % concentration of the undeprotonated [Cu^{II}(LH)]$^{2+}$ complex; solid line: % concentration of the deprotonated [Cu^{II}(L)]$^{+}$ species (off right vertical axis), (b) symbols: absorbance of the bands centred at 350 nm, [Cu^{II}(LH)]$^{2+}$ (right vertical axis) and at 450 nm, [Cu^{II}(L)]$^{+}$ (left vertical axis). Figure adapted from Ref. [34].

unit, which, on deprotonation of the N–H fragment, has assumed a partial negative charge. The process is pictorially illustrated in Scheme 9.

A similar behavior was noted with complex $[\mathbf{15}]^{2+}$. In fact, on titrating a DMSO solution of the $[\mathbf{15}](ClO_4)_2$ salt, drastic spectral modifications were observed, as shown in Fig. 11a.

In particular, acetate addition induced a 110 nm red-shift of the charge transfer band centered at 340 nm, strongly indicative of the deprotonation of the amide N–H fragment. Best fitting of the titration data, using a non-linear least-squares procedure, over the 250–550 nm interval, was obtained upon assuming the occurrence of an equilibrium of type (1), to which a $\log K = 4.81 \pm 0.03$ corresponded. Such a neutralization constant is 0.5 log unit higher than that observed with the cyanophenyl derivative $[\mathbf{16}]^{2+}$, a behavior which reflects the more pronounced electron-withdrawing tendencies of the nitrophenyl substituent. Also in the case of system $[\mathbf{15}]^{2+}$, the absorbance of the two bands was found to fit well the calculated concentration profiles of the undeprotonated and deprotonated $[Cu^{II}(LH)]^{2+}$ and $[Cu^{II}(L)]^{+}$ complexes. However, for system $[\mathbf{15}]^{2+}$ the hypothesis of the carbonyl oxygen binding through a scorpionate mode could not be corroborated by d–d spectra because the tail of the intense absorption band of the nitrophenyl subunit obscured the wavelength interval in which metal-centered transitions of $Cu^{II}(azacyclam)^{2+}$ complexes are typically observed.

6. Conclusion

Busch [2] and Curtis [43] during the 1960s introduced metal templates for synthesizing tetra-aza macrocycles (rings). The metal template approach has been more recently used to obtain molecular systems of increasing complexity and sophistication. However, simple tetra-aza macrocycles, in particular cyclam-like ligands, still maintain their appeal and can provide novel and promising functions. In particular, cyclam complexes on one side exhibit a unique kinetic stability, which excludes demetalation even in rather drastic conditions, and, on the other side, provide two axial coordination sites for interaction with any substrate. This makes cyclam complexes secure and versatile players in electron transfer processes, catalysis, and anion recognition. The azacylam template approach affords a convenient route to the synthesis of bifunctional systems, in which the interaction of a given substrate with the metal center is controlled by the appended functionality, whose nature and distance can be modified by design.

Acknowledgements

We thank the University of Pavia and the Italian Ministry of University and Research for financial support.

References

[1] J. McCleverty, T.J. Meyer (Eds.), Comprehensive Coordination Chemistry II, From Biology to Nanotechnology, Elsevier, 2003.
[2] M.C. Thompson, D.H. Busch, J. Am. Chem. Soc. 86 (1964) 3651.
[3] J.L. Karn, D.H. Busch, Nature 211 (1966) 160.
[4] J.L. Karn, D.H. Busch, Inorg. Chem. 8 (1969) 1149.
[5] The origin of the abbreviations CR and CRH is not straightforward. Professor Busch kindly told one of us (L.F.) that CR derives from the surname of his former student J.D. Curry, who, in the Busch's lab, was the first to study metal template reactions of 2,6-diacetylpyridine with linear polyamines (in particular tetramines, which, thanks to the template effect exerted by Fe^{III}, gave penta-aza-macrocyclic complexes) [6,7]. The abbreviation CR was then extended to the Karn's macrocycle obtained from triamine 3, to give the Ni^{II} tetra-aza-macrocyclic complex **4**. CRH refers to the hydrogenated ligand.
[6] J.D. Curry, Ph.D. Thesis, The Ohio State University, 1964.
[7] J.D. Curry, D.H. Busch, J. Am. Chem. Soc. 86 (1964) 592.
[8] M.G.B. Drew, S. Hollis, Acta Crystallogr. Sect. B: Struct. Crystallogr. Cryst. Chem. 36 (1980) 718.
[9] R. Dewar, E. Fleischer, Nature 222 (1969) 372.
[10] (a) E.K. Barefield, Inorg. Chem. 11 (1972) 2273;
(b) E.K. Barefield, F. Wagner, A.W. Herlinger, A.R. Dahl, Inorg. Synth. 16 (1975) 220.
[11] L. Fabbrizzi, Comments Inorg. Chem. 4 (1985) 33.
[12] C. Bisi Castellani, L. Fabbrizzi, M. Licchelli, A. Perotti, A. Poggi, J. Chem. Soc.: Chem. Commun. (1984) 806.
[13] T. Ito, H. Ito, K. Toriumi, Chem. Lett. (1981) 1101.
[14] M. Pesavento, A. Profumo, T. Soldi, L. Fabbrizzi, Inorg. Chem. 24 (1985) 3873.
[15] E.K. Barefield, M.T. Mocella, Inorg. Chem. 12 (1973) 2829.
[16] F.V. LoVecchio, E.S. Gore, D.H. Busch, J. Am. Chem. Soc. 96 (1974) 3109.
[17] L. Fabbrizzi, Pure Appl. Chem. 61 (1989) 1569.
[18] L. Fabbrizzi, M. Licchelli, P. Pallavicini, Acc. Chem. Res. 32 (1999) 846.
[19] L. Fabbrizzi, F. Gatti, P. Pallavicini, E. Zambarbieri, Chem.: Eur. J. 5 (5) (1999) 682.
[20] G. De Santis, M. Di Casa, M. Mariani, B. Seghi, L. Fabbrizzi, J. Am. Chem. Soc. 111 (1989) 2422.
[21] M. Ciampolini, L. Fabbrizzi, M. Licchelli, A. Perotti, F. Pezzini, A. Poggi, Inorg. Chem. 25 (1986) 4131.
[22] I.I. Creaser, J.M. Harrowfield, A.J. Herlt, A.M. Sargeson, J. Springborg, R.J. Geue, M.R. Snow, J. Am. Chem. Soc. 99 (1977) 3181.
[23] R.J. Geue, T.W. Hambley, J.M. Harrowfield, A.M. Sargeson, M.R. Snow, J. Am. Chem. Soc. 106 (1984) 5478.
[24] P. Comba, N.F. Curtis, G.A. Lawrance, A.M. Sargeson, B.W. Skelton, A.H. White, Inorg. Chem. 25 (1986) 4260.
[25] M. Paik Suh, S.-G. Kangl, Inorg. Chem. 27 (1988) 2544.
[26] A. De Blas, G. De Santis, L. Fabbrizzi, M. Licchelli, A.M. Manotti Lanfredi, P. Morosini, P. Pallavicini, F. Ugozzoli, J. Chem. Soc.: Dalton Trans. (1993) 1411.
[27] F. Abbà, G. De Santis, L. Fabbrizzi, M. Licchelli, A.M. Manotti Lanfredi, P. Pallavicini, A. Poggi, F. Ugozzoli, Inorg. Chem. 33 (1994) 1366.
[28] P.A. Tasker, L. Sklar, J. Cryst. Mol. Struct. 5 (1975) 329.
[29] V.J. Thöm, J.C.A. Boeyens, G.J. McDougall, R.D. Hancock, J. Am. Chem. Soc. 106 (1984) 3198.
[30] K.R. Adam, I.M. Atkinson, L.F. Lindoy, Inorg. Chem. 36 (1997) 480.
[31] A. De Blas, G. De Santis, L. Fabbrizzi, M. Licchelli, C. Mangano, P. Pallavicini, Inorg. Chim. Acta 115 (1992) 202.
[32] G. De Santis, L. Fabbrizzi, M. Licchelli, C. Mangano, P. Pallavicini, Inorg. Chim. Acta 214 (1993) 193.
[33] G. De Santis, L. Fabbrizzi, M. Licchelli, N. Sardone, A.H. Velders, Chem.: Eur. J. 2 (1996) 1243.
[34] M. Boiocchi, L. Fabbrizzi, M. Garolfi, M. Licchelli, L. Mosca, C. Zanini, Chem.: Eur. J. 15 (2009) 11288.
[35] (a) P.A. Gale, Amide and urea based anion receptors, in: Encyclopedia of Supramolecular Chemistry, Marcel Dekker, New York, 2004, pp. 31–41;
(b) K. Choi, A.D. Hamilton, J. Am. Chem. Soc. 125 (2003) 10241;
(c) S.O. Kang, J.M. Llinares, D. Powell, D. VanderVelde, K. Bowman-James, J. Am. Chem. Soc. 125 (2003) 10152;
(d) S. Otto, S. Kubik, J. Am. Chem. Soc. 125 (2003) 7804;
(e) C.R. Bondy, S.J. Loeb, Coord. Chem. Rev. 240 (2003) 77;
(f) S.O. Kang, M.A. Hossain, K. Bowman-James, Coord. Chem. Rev. 250 (2006) 3038.
[36] J.L. Sessler, P.A. Gale, W.-S. Cho, Anion Receptor Chemistry, Royal Society of Chemistry, Cambridge, UK, 2006.
[37] V. Amendola, D. Esteban-Gómez, L. Fabbrizzi, M. Licchelli, Acc. Chem. Res. 39 (2006) 343.
[38] K. Bowman-James, Acc. Chem. Res. 38 (2005) 671.
[39] M. Boiocchi, L. Del Boca, D. Esteban-Gómez, L. Fabbrizzi, M. Licchelli, E. Monzani, J. Am. Chem. Soc. 126 (2004) 16507.
[40] M. Boiocchi, L. Del Boca, D. Esteban-Gómez, L. Fabbrizzi, M. Licchelli, E. Monzani, Chem.: Eur. J. 11 (2005) 3097.
[41] D. Esteban-Gómez, L. Fabbrizzi, M. Licchelli, E. Monzani, Org. Biomol. Chem. 3 (2005) 1495.
[42] F.G. Bordwell, Acc. Chem. Res. 21 (1988) 456.
[43] N.F. Curtis, J. Chem. Soc. (1964) 2644.